Supplementary Figures

Peck *et al*. **3D functional genomics screens identify CREBBP as a targetable driver in aggressive triple negative breast cancer**

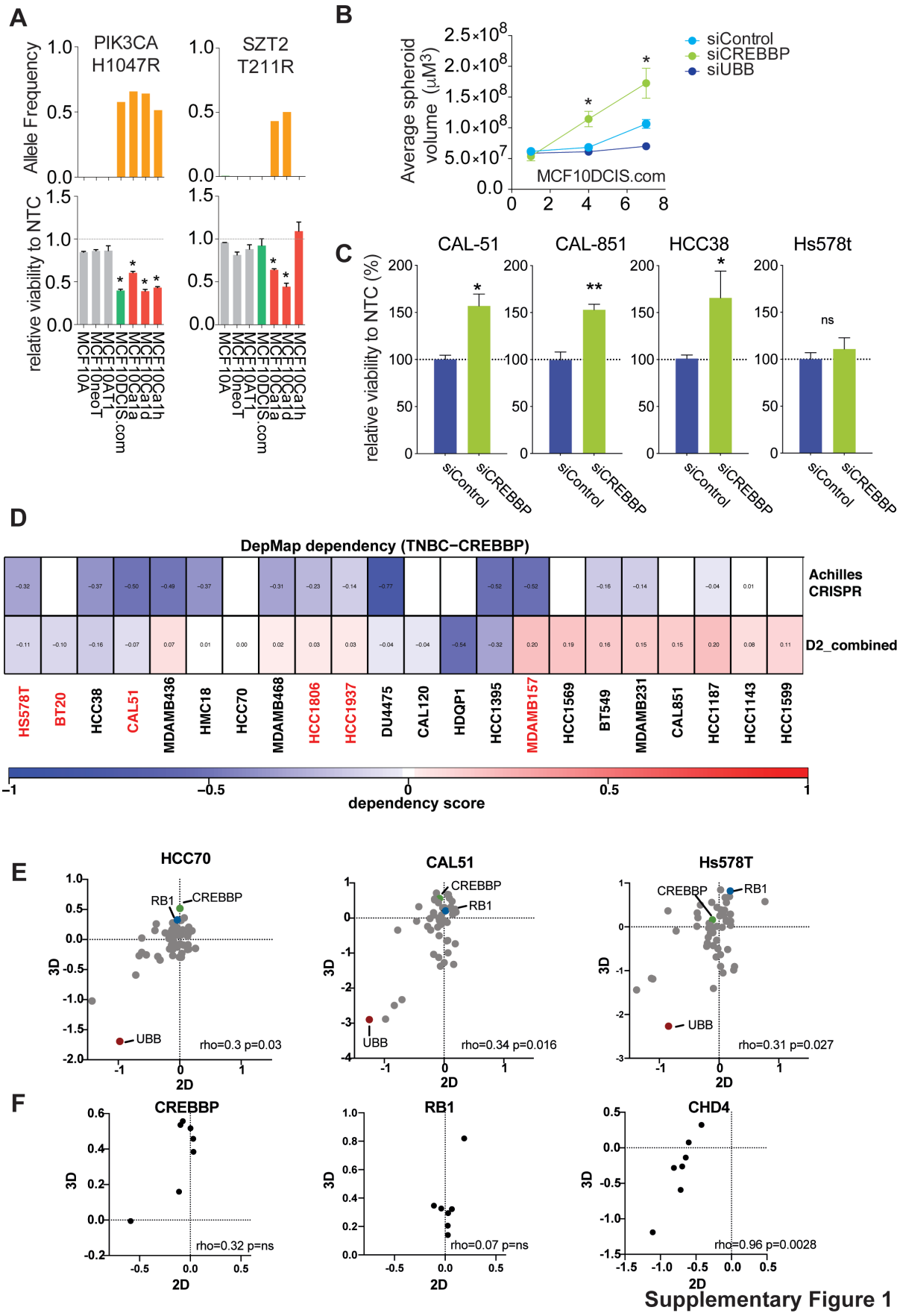

Supplementary Figure 1

Supplementary Figure 1: Growth advantage upon CREBBP silencing is 3D specific.

(A) Gene allelic frequencies and cell viability after gene silencing of PIK3CA and SZT2 in the MCF10 progression series from the initial screen. (B) Relative growth of MCF10DCIS.com cell line spheroids after CREBBP silencing. (C) Bar chart depicting relative viability of spheroids after CREBBP silencing in additional TNBC cell lines. (D) Heatmap of dependency scores of CREBBP silencing in TNBC cell lines from DepMap. Cell lines utilised in the TNBC validation screen are highlighted in red text. (E) Scatter plots of the spheroid viability of TNBC cell lines under 2D and 3D conditions with the top fifty siRNAs relative to non-targeting control siRNA (NTC), depicting CREBBP and RB1 as 3D specific hits. (2D data taken from DepMap). UBB is depicted as a killing control consistent in both 2D and 3D data. (F) Scatter plots of 2D versus 3D viability across the TNBC cell line series used in the validation screen highlighting lack of correlation between 2D and 3D for CREBBP and RB1 silencing.

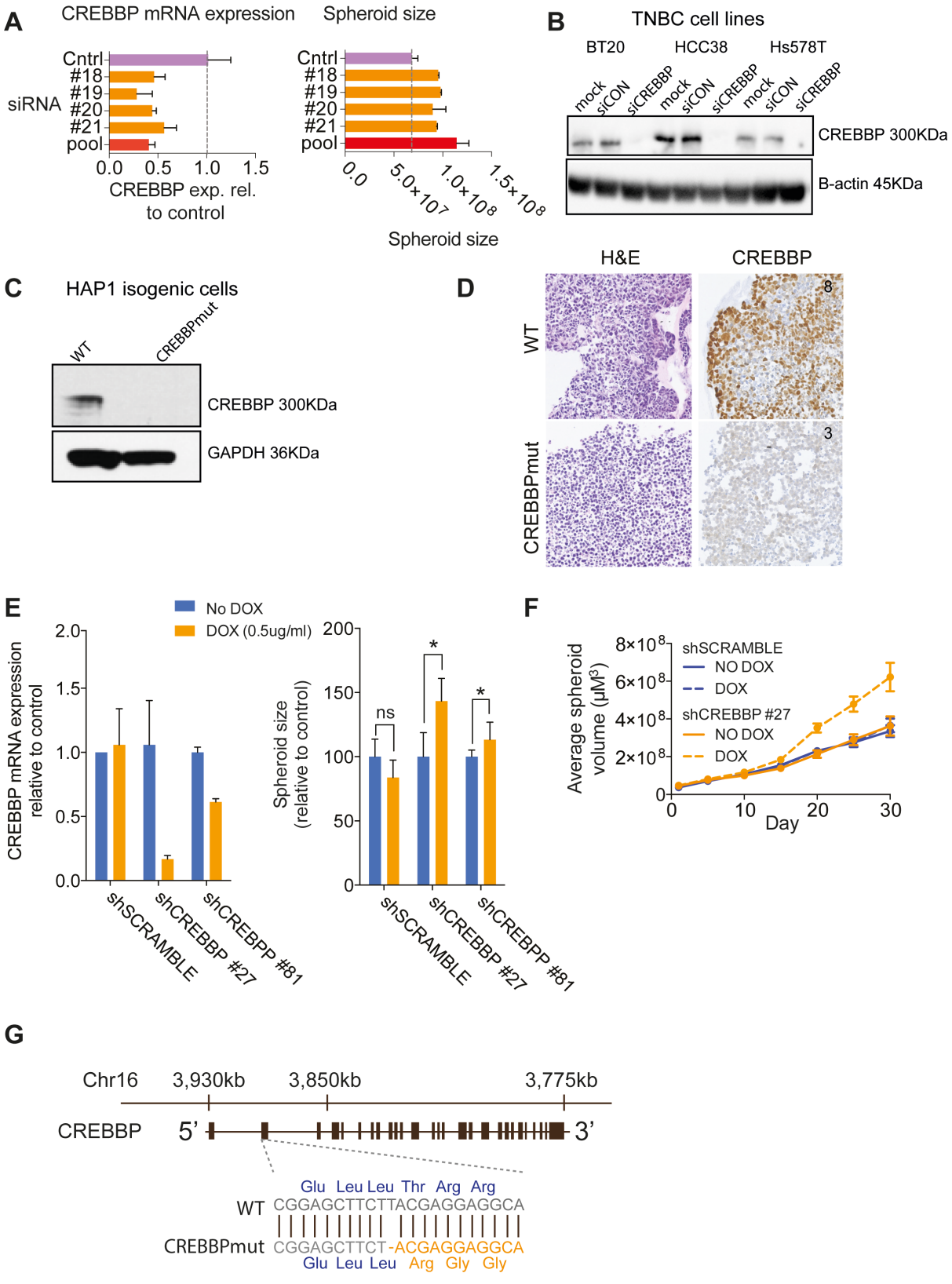

Supplementary Figure 2

Supplementary Figure 2: Deconvolution of CREBBP targeting tools.

A) Bar chart depicting relative mRNA expression of CREBBP and spheroid size of MCF10DCIS.com spheroids reverse transfected with CREBBP or non-targeting control siRNA for five days. (B) Western blot of CREBBP and B-actin loading control in TNBC cell lines with CREBBP siRNA smartpool, highlighting loss of CREBBP protein expression. (C) Western blot of CREBBP and GAPDH loading control in HAP1 isogenic CREBBPmut and WT cell lines, highlighting loss of CREBBP protein expression in CREBBPmut CRISPR knockout cells. (D) H&E and IHC of HAP1 CREBBPmut and WT cells. Allred scores are depicted. (E) Bar chart depicting relative mRNA expression of CREBBP and spheroid viability of MCF10DCIS.com cell lines expressing doxycycline-inducible shRNA constructs against *CREBBP* (shCREBBP #27 and #81) and a non-targeting control (shSCRAMBLE). Spheroids were treated with doxycycline (0.5ug/ml) from day one every 3 days. Spheroids were pooled and snap frozen at day seven, RNA was extracted and CREBBP expression was quantified using RT-PCR. (F) Relative spheroid size over time of MCF10DCIS.com cells with shCREBBP #27 and non-targeting control (shSCRAMBLE). (G) Schematic of CRISPR engineered 1bp deletion in HAP1 cells.

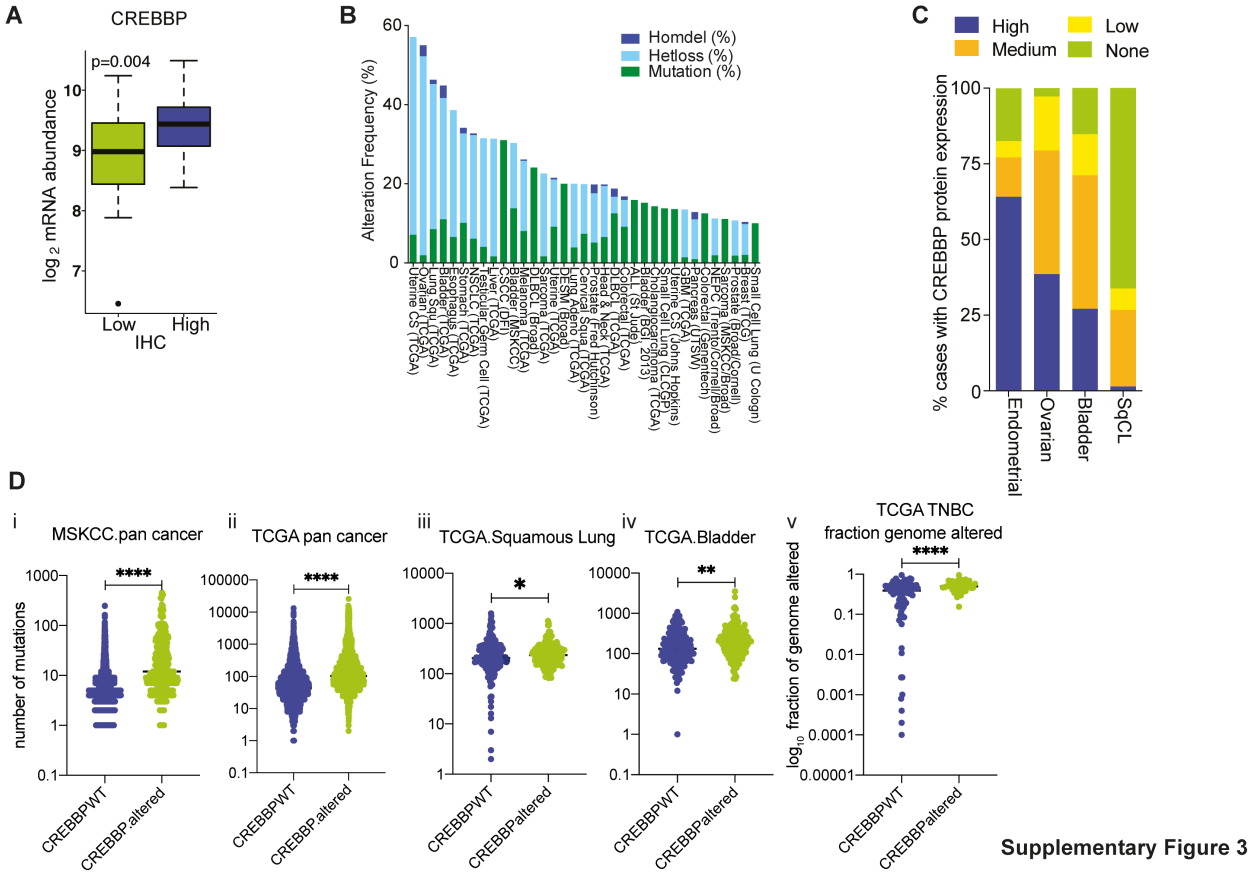

Supplementary Figure 3

Supplementary Figure 3: CREBBP is altered in multiple tumour types.

(A) Box and whiskers plot of relative mRNA expression of primary TNBC patients from the 'Belgrade" series stratified by CREBBP protein expression, highlighting a significant correlation between mRNA and protein. (B) Frequency bar charts of alterations in CREBBP in multiple solid tumours (TCGA from cBioportal). (C) Bar chart depicting frequency of CREBBP protein expression from TMA assessment in endometrial, ovarian, bladder and squamous cell lung cancer. (D) Scatter plot of number of mutations identified in CREBBPaltered versus WT primary tumours from i) MSKCC and ii) TCGA pancancer analyses; iii) squamous lung cancers (TCGA), iv) bladder cancers (TCGA) and v) fraction of the genome altered in TNBC.

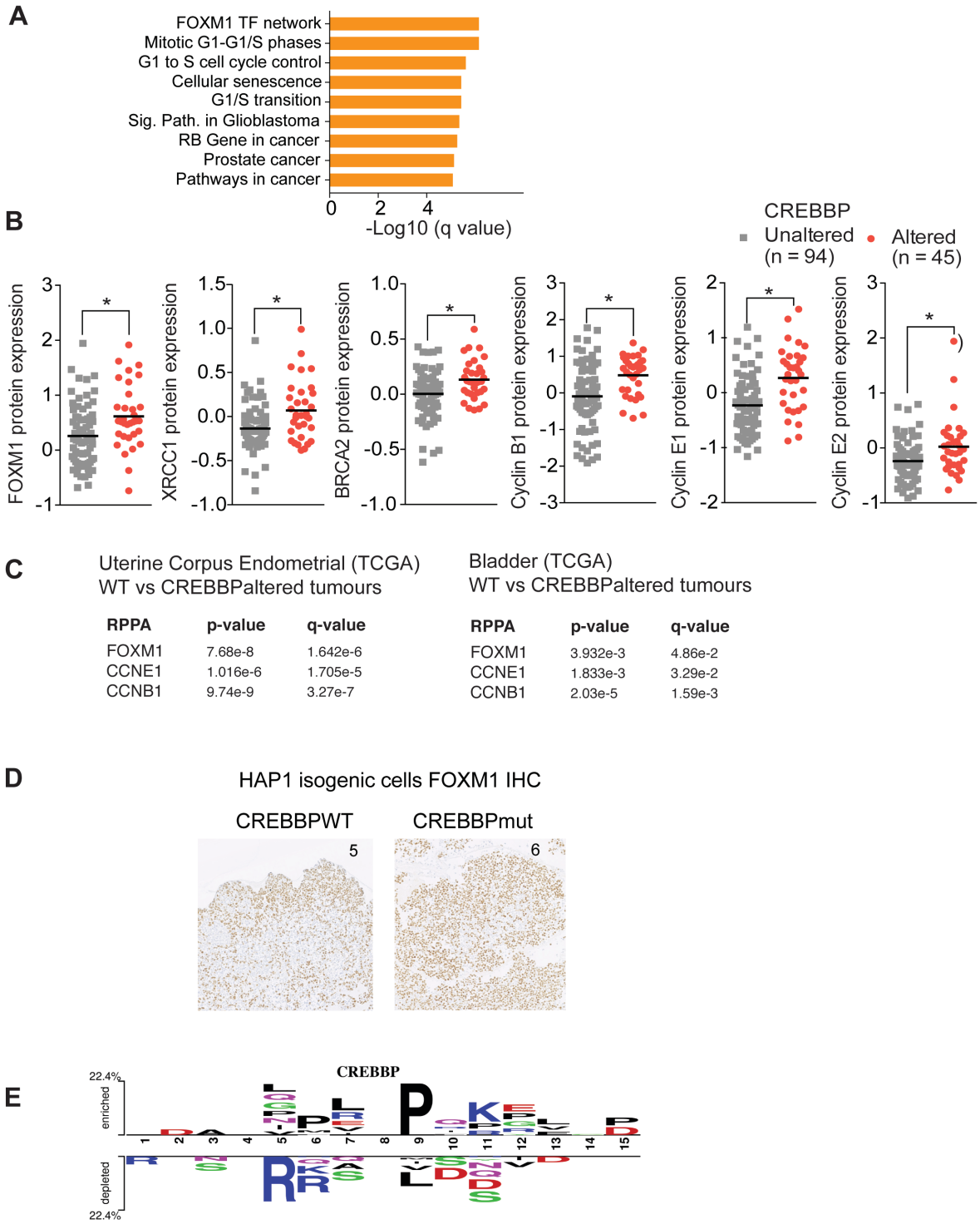

Supplementary Figure 4

Supplementary Figure 4: CREBBP loss is associated with increase in FOXM1 expression.

(A) Bar chart depicting significantly enriched pathways plotted against –log10 q-value (y-axis) from pathway enrichment analysis of RPPA data of CREBBPaltered TNBC vs WT from TCGA data. (B) Scatter dot plot depicting a significant association of protein expression of FOXM1 and known target genes between CREBBPaltered versus WT TNBC's from TCGA. Significant alterations in protein expression are highlighted and individual tumours are highlight for WT (grey) and CREBBPaltered (red) tumours (*q value <0.1. ** <0.01). (C) Table showing the significant associations of FOXM1 protein expression and downstream target genes from RPPA data of FOXM1, CCNB1 and CCNE1 in uterine and bladder cancers (TCGA). P and q values are shown. (D) FOXM1 protein expression detected by immunohistochemistry in HAP1 WT and CREBBPmut spheroids showing increased expression in CREBBPmut cells. Text depicts IHC quantification (Allred scores). (E) Kinase motif analysis depicting global enrichment of CDK4/6 motifs in CREBBPmut HAP1 spheroids compared to WT.

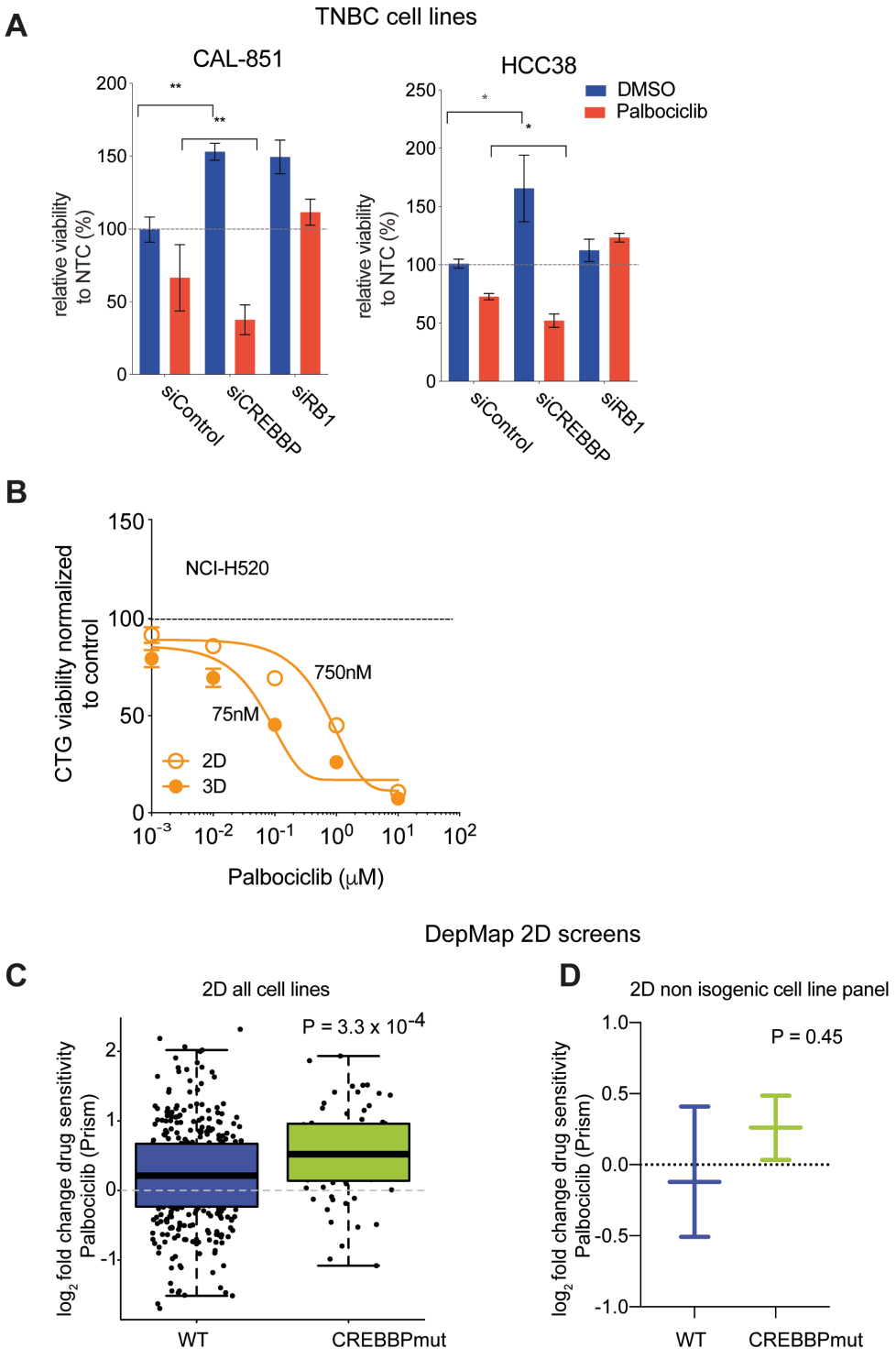

Supplementary Figure 5

Supplementary Figure 5: CREBBP loss is associated with CDK4/6i sensitivity in 3D

(A) Barplot of TNBC cell lines showing increase growth when CREBBP is silenced and subsequent increased sensitivity to Palbociclib compared to siControl. Note RB1 silencing results in resistance to Palbociclib. (B) Dose response curves of lung cancer cell line NCI-H520 harbouring an endogenous CREBBP mutation in 2D and 3D, highlighting increased sensitivity to Palbociclib in 3D. (C) Box and whiskers plots of pan cancer cell line sensitivity to Palbociclib stratified on CREBBP mutation status, taken from DepMap. Note decrease sensitivity in CREBBPmut cell lines compared to CREBBPWT grown in 2D. (D) Box and whiskers plots of the cancer cell line panel grown in 2D (used in Figure 5) and sensitivity to Palbociclib stratified on CREBBP mutation status. Data taken from DepMap.

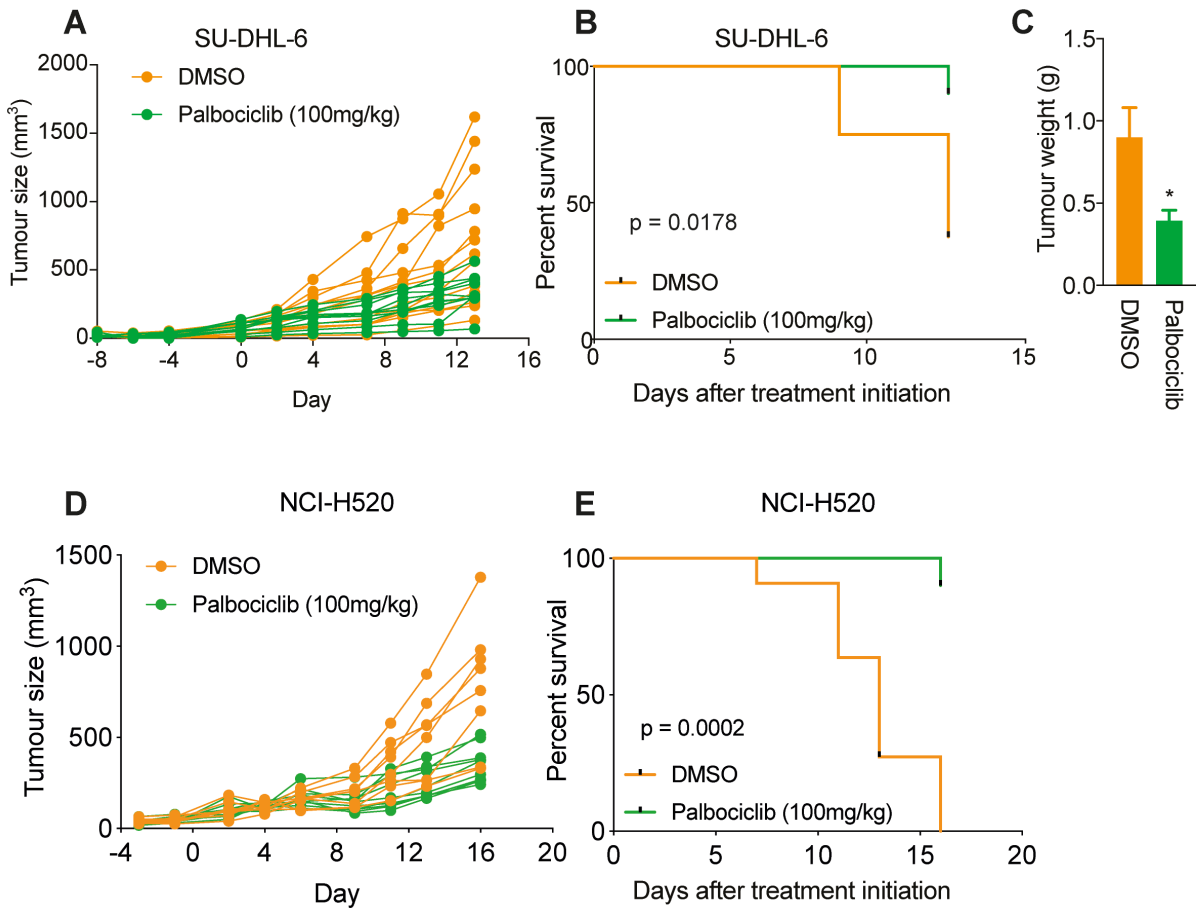

Supplementary Figure 6

Supplementary Figure 6: Palbociclib treatment reduces CREBBPaltered xenograft growth.

(A) Chart depicting individual animal tumour volumes of the therapeutic response to Palbociclib treatment in NSG mice bearing CREBBP–mutant SU-DHL-6 tumours over time. Once tumours reached 100-150mm^3 they were equally stratified into vehicle and Palbociclib (100mg/kg) treatment arms and tumour sizes were measured with callipers every 2-3 days. Tumour volumes after the initiation of treatment are shown. (B) Kaplan-Meier curves of SU-DHL-6 tumours depicting an increase in survival in animals treated with Palbociclib, (HR=7.558, 95% CI= 1.474 to 38.75, logrank test). (C) Bar

chart showing SU-DHL-6 tumour weights. (D) Chart depicting individual animal tumour volumes of the therapeutic response to Palbociclib treatment in immunocompromised mice bearing CREBBP–mutant NCI-H520 tumours over time. Once tumours reached 100-150mm^3 they were equally stratified into vehicle and Palbociclib (100mg/kg) treatment arms and tumour sizes were measured with calipers every 2-3 days. Tumour volumes after the initiation of treatment are shown. (E) Kaplan-Meier curves of NCI-H520 tumours depicting an increase in survival in animals treated with Palbociclib, (HR=16.0, 95% CI= 3.797 to 67.44, logrank test).

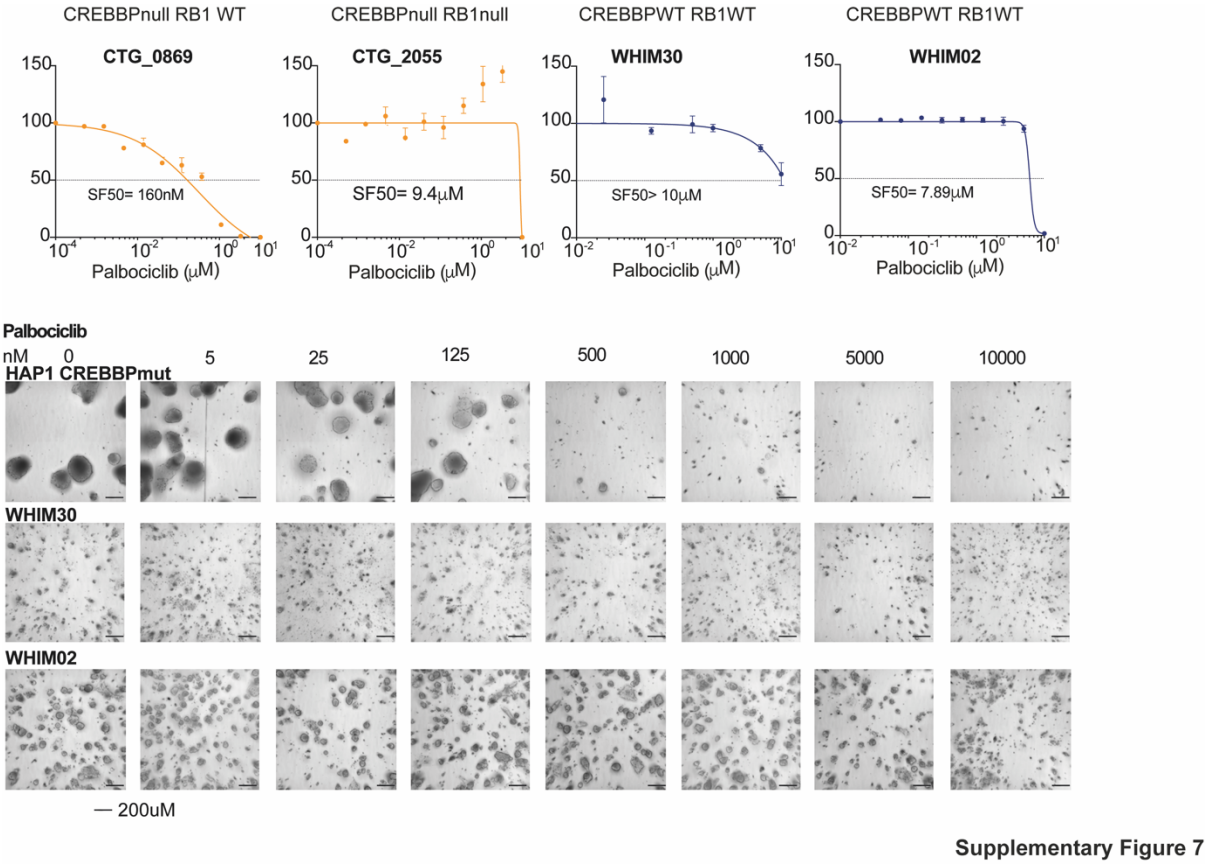

Supplementary Figure 7: Palbociclib treatment in TNBC patient derived organoids

Dose response curve of TNBC PDX's grown *ex-vivo* and treated with increasing concentrations of Palbociclib for 14 days. Representative organoid images are shown (related to Figure 6E).

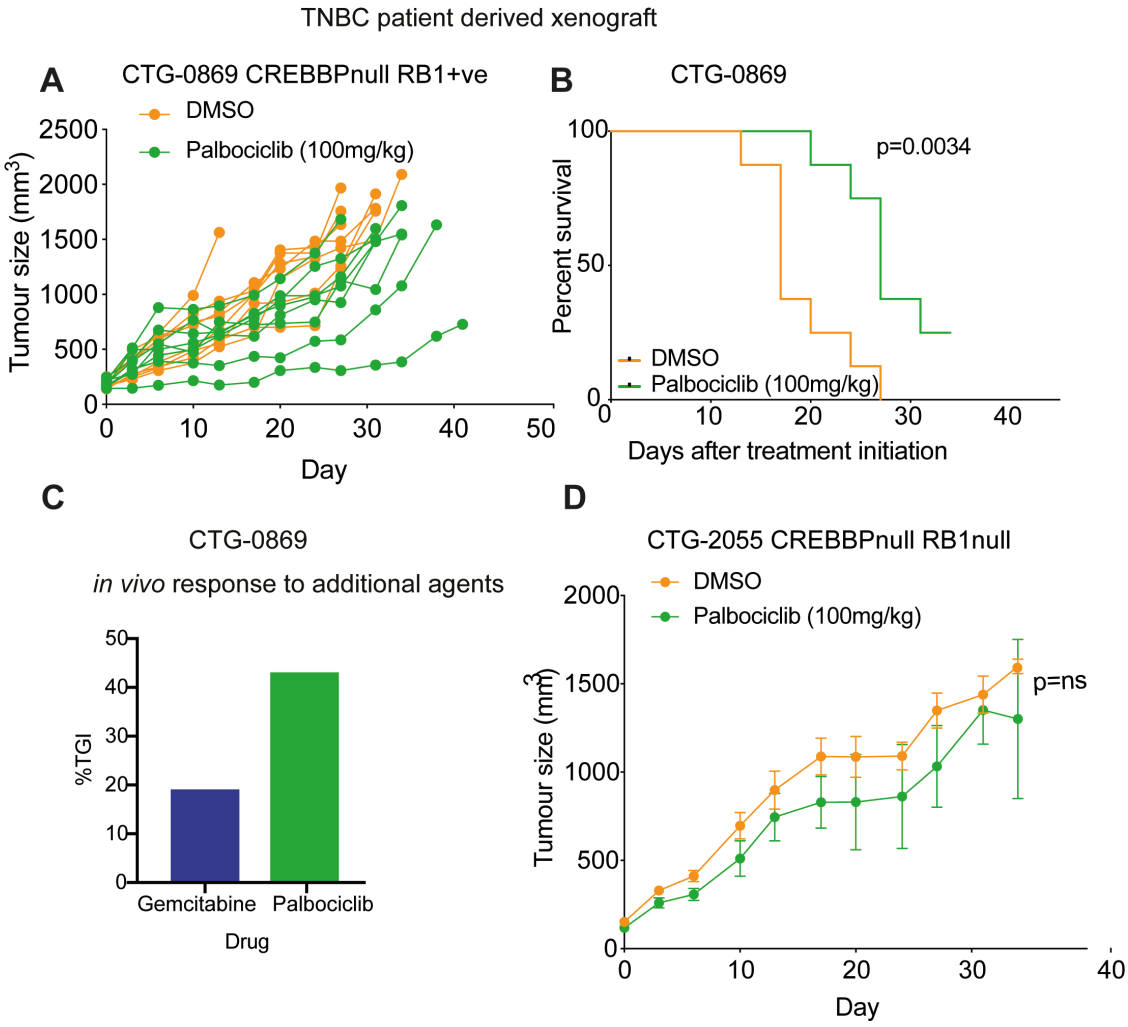

Supplementary Figure 8

Supplementary Figure 8: Palbociclib treatment reduces CREBBPaltered TNBC growth.

(A) Chart depicting individual animal tumour volumes of the therapeutic response to Palbociclib treatment in immunocompromised mice bearing CREBBPnull TNBC PDX CTG-0869 tumours over time. Once tumours showed an increase in growth they were equally stratified into vehicle and Palbociclib (100mg/kg) treatment arms and tumour sizes were measured with calipers every 2-3 days. Tumour volumes after the initiation of treatment are shown. (B) Kaplan-Meier curves of CTG-0869 tumours depicting an increase in survival in animals treated with Palbociclib, (HR=3.221, 95% CI= 1.019 to

10.18, logrank test). (C) Chart depicting tumour growth inhibition (TGI) as percentage of DMSO treated mice bearing CTG-0869 TNBC xenografts treated with Gemcitabine (n=8) and Palbociclib. (D) Chart depicting CTG-2055 tumour volume of the therapeutic response to Palbociclib treatment in immunocompromised mice showing a no significant inhibition of tumour volume upon treatment with CDK4/6i. Tumour volumes after the initiation of treatment are shown.